Controlling Particle Size During Anatase Precipitation

Sekhar Sathyamoorthy and Geoff D. Moggridge
Dept. of Chemical Engineering, Cambridge University, Pembroke Street, Cambridge CB2 3RA, U.K.

Michael J. Hounslow
Dept. of Chemical and Process Engineering, University of Sheffield, Mappin Street, Sheffield S1 3JD, U.K.

Titanium dioxide particles in the form of anatase are precipitated from concentrated titanyl sulfate solution in the sulfate process, which are then recovered by a filtration process downstream of the precipitation stage. A previous study by Sathyamoorthy et al. showed that the final anatase particles are aggregates (1-2 μm) consisting of numerous crystals (7–8 nm) arranged in primary agglomerates (60–100 nm). Pigment quality is determined by crystal and primary agglomerate size. One way of improving filtration rate is by the formation of larger aggregates, while maintaining the crystal and primary agglomerate size at optimum values. In a new seeding procedure proposed, the controlled inoculation of seeds used in industry is combined with a new type of seed (Large Seeds). The new seeding procedure has the potential to increase downstream filtration efficiency by increasing aggregate size, while maintaining crystal and primary agglomerate sizes close to the values correctly obtained in industry. High yield in the precipitation process is also maintained.

Introduction

Titanium dioxide is mainly known for its good pigment properties. Apart from its well-known application in paints, it is also used in the manufacture of paper, fibers, cosmetics, sunscreen products, toothpaste, and foodstuffs. One route to titanium dioxide production is via the sulfate process (Barksdale, 1966). This is the main production method used outside North America (Tioxide, 1992).

Ilmenite, the titanium-dioxide-bearing ore is dissolved in concentrated sulfuric acid. The resulting titanyl sulfate solution is purified by the removal of iron. Precipitation of titanium dioxide in the form of anatase occurs from concentrated titanyl sulfate solution in batch stirred tanks. The anatase slurry is then filtered to recover the solid particles. The final processing step involves calcination at 900°C, at which temperature anatase transforms to rutile, which is the final pigment form. The precipitation of anatase particles is crucial to the process, because the optical properties of the pigment are first established here, the most important property being particle size.

Correspondence concerning this article should be addressed to G. D. Moggridge.

Achieving an optimum crystal-size range is desirable for pigment applications. In order to most efficiently reflect visible wavelengths (0.4–0.7 μm), the particle size of titanium dioxide pigments must be controlled at about half those dimensions, or 0.2–0.4 μm (Patton, 1973).

In the sulfate process, the solid–liquid separation of the anatase slurry after precipitation is carried out by the cake filtration technique. The structure of the filter cake determines the efficiency of the filtration process. Larger anatase particles allow the formation of a more porous filter cake, improving filtrability of the slurry and reducing filtration time in the process. The key factors in industry are process economy and the high quality of the final product.

Particle Formation During Anatase Precipitation

A comprehensive study of the particle formation process during precipitation has been described by Sathyamoorthy et al. (2001a,b). Seeds were found to be important in accelerating the precipitation process. Seeds compose 4–5 nm anatase crystals. These seeds induce the formation of primary agglomerates (approximately 60–100 nm), which aggregate to

form particles (aggregates) of approximately 1–2 μm. Crystal size at the end of precipitation was found to be between 7 and 8 nm. Sathyamoorthy et al. (2001a) defined a primary agglomerate to be a tightly bound group of crystals. Crystals within a primary agglomerate are held together by solid bridges of crystalline material and cannot be separated by the addition of barium chloride. It is likely that all the crystals within a single primary agglomerate were originally formed by secondary nucleation events occurring on the surfaces of other crystals present in the same agglomerate. An aggregate was defined as a more loosely bound collection of primary agglomerates. The primary agglomerates within an aggregate are held together only by weak bridges and/or surface attractions. The addition of barium chloride sufficiently modifies the surfaces of anatase (by scavenging sulfate ions from solution) that the primary agglomerates within an aggregate separate. Unfortunately, the term "aggregate" is used differently by other investigators. In the field of colloid science, the term "aggregate" usually refers to permanent, nonredispersible entities that are defined here as "agglomerates." Colloid scientist make use the term "floc" instead of "aggregate" (as used in this article) to define loosely bound entities.

The rate of precipitation in dependent on secondary nucleation, and can be dramatically enhanced by increasing the amount of seeds inoculated. Earlier work on particle size during anatase precipitation has been reported by Duncan et al. (1976), Santacesaria et al. (1986), and Raskopf et al. (1999).

The final size of crystals and primary agglomerates are crucial in determining pigment quality (Edwards, personal communication, 1999). Therefore, these two length scales must be controlled within an optimum range during precipitation. On the other hand, the size of aggregates dictates the efficiency of the filtration process downstream of anatase precipitation, but does not affect final pigment quality (Chung et al., 1999). Thus, the formation of larger aggregates is favorable to the economy of the process. The main focus of the work presented in this article is on maintaining crystal and primary agglomerate size within the optimum range achieved in industry, maintaining high yield in the process, and at the same time increasing the size of aggregates and thereby enhancing filtration efficiency.

This article describes the possibility of using an alternative, readily available source of seeding material. Anatase particles from a previous run were used as seeds in the recovery of titanium dioxide from fresh titanyl sulfate solution. Unlike the seeds used in industry, the seeds we made remained in the micron-size range when inoculated into titanyl sulfate solution. A new seeding procedure was developed, and the slurry obtained was tested by simple filtration experiments.

In a recent study, Sathyamoorthy et al. (2001b) investigated the influence of stirrer speed on particle size during anatase precipitation in a mechanically stirred vessel. It was found that crystal size, agglomerate size, and yield were essentially unaffected by stirrer speed, but that aggregate size decreased as stirrer speed was increased; the range of aggregate size attainable remained fairly limited.

Another factor that could influence aggregate size is the effect of seeding during precipitation. In industry seeds are used to obtain a high recovery rate and control of the particles-size distribution (PSD). An investigation into the influence of seeds on aggregate size has been documented by Sathyamoorthy et al. (2001a). The final mean size of the aggregates was not significantly influenced by changing the seeding volume used.

Theory of Cake Filtration

In cake filtration the slurry is forced through a porous medium of low resistance, on which the solid material is retained, while the liquid passes through. A cake of solid particles with a complex pore structure is soon established on the porous medium. This filter cake retains other solid particles and forms the main resistance to the flow of slurry. The efficiency of the cake filtration process depends on cake permeability, pore size, particle size, and compressibility (Cain, 1990).

The macroscopic properties of the filter cake are largely dependent on the properties of the solid particles in the slurry. One of the most important parameters of both slurry and filter cake is the particle-size distribution. In cake filtration, cake permeability is often regarded as the most convenient characterization parameter.

Mydlarz and Jones (1989), Svarosvsky (1990), and Ranjan and Hogg (1996) have analyzed cake filtration using the Carman-Kozeny equation and found it to work reasonably well over a limited range of experimental parameters. They found that cake permeability increased with increasing particle size for monodisperse suspensions. In deriving the Carman-Kozeny equation, it is assumed that all particles are spherical. In our case, although the primary agglomerates are roughly spherical, the aggregates appear more like "cauliflower florets." The aggregates cannot therefore be expected to arrange themselves in the filter cake as would spherical particles, and so the Carman-Kozeny equation is unlikely to give good results. For this reason we have analyzed our filtration data using a method based on recent work described by Meeten (2000). An outline of the mathematical formulation is given here.

The simple mathematical description of a filtration process for an incompressible cake is often based on Darcy's law (Mydlarz and Jones, 1989), shown in Eq. 1. This gives a definition of cake permeability, k:

$$\frac{dQ}{dt} = \frac{kP}{\eta L}. \tag{1}$$

Following the work of Meeten (1993) and Akers and Ward (1977), Meeten (2000) derived an expression for desorptivity (Eq. 2) for an incompressible cake:

$$S = \left(\frac{2kP}{\eta G}\right)^{0.5}, \tag{2}$$

where $G = \phi/(\phi_{\text{cake}} - \phi) = (\text{cake volume})/(\text{filtrate volume})$, which for an incompressible cake is constant throughout the filtration process.

Further analysis by Meeten produced an expression identical in form to the formula proposed by Ruth et al. in 1933. The so-called Ruth relation is given as

$$t = t_0 + bV + cV^2, \tag{3}$$

where $b = \eta R A^{-1} P^{-1}$ and $c = A^{-2} S^{-2}$; t_o, b, and c are determined by curve fitting a second-order polynomial to a plot of time vs. cumulative volume of filtrate; S, desorptivity, is calculated from the value of c and the surface area of the porous media. Cake permeability, k, is then determined from the plot of S vs. $P^{0.5}$, Eq. 2; S and R are both assumed to be constant over time during a given experiment; and R should also be pressure independent, and S also will be for an incompressible cake. This type of analysis allows the effect of the inherent filter medium hydraulic resistance, R, to be separated from the cake permeability, k.

In the filtration of fine particles such as anatase, the influence of pH on the surface charges of the particles and the resulting network formation through physicochemical interactions in the filter cake should be a prime consideration. Koenders and Wakeman (1996) determined the isoelectric point for anatase particles (produced by a similar precipitation route to that used in our work) and found that it was close to pH 3.4. Close to the isoelectric point the rate of filtration varied considerably with pH (pH 2 to pH 4). The filtration rate reached its maximum value at pH 3.4. Thereafter, filtration rate reduced as the modulus of the zeta potential was increased up to pH 5.5. At pH greater than 5.5, the filtration rate did not change significantly, corresponding to the small change in zeta potential when the pH was greater than 5.5. Hence, the modulus of zeta potential caused by changes in the pH of the slurry affects the filtration efficiency of anatase slurry. This was an important consideration taken into account in the preparation of anatase slurry for filtration work described in this article (see Experimental section).

Experimental Studies

Batch mode experiments were carried out in a mechanically stirred tank of 1-L capacity. The vessel is described in detail by Sathyamoorthy et al. (2000b). Five hundred mL of concentrated titanyl sulfate (black liquor) obtained from an industrial source was used. This solution consists of 253.43 g/L titanium dioxide and 464.10 g/L sulfuric acid. The industrial fluid also includes 30.56 g/L Fe^{2+} in aqueous form and trace amounts of other impurities. One function of the industrial digestion and precipitation process is the removal of these impurities (Tioxide, 1992).

Industrial Seeds are made from the reaction of titanium tetrachloride and sodium hydroxide. Industrial Seeds were obtained from the same industrial source. Titanium dioxide concentration in Industrial Seeds was 43.6 g/L. Inoculation of 54 mL Industrial Seeds is equivalent to seeding on a basis of 1.8% wt of titanium dioxide in the vessel. Industrial Seeds compose particles with mean size of 10 μm. These large particles break into anatase crystals of 4–8 nm, when innoculated into black liquor (Sathyamoorthy et al., 2001a).

A different type of seed was also used in the experiments. These seeds were obtained from the final product of a precipitation run. Fresh titanyl sulfate, inoculated with 54 mL of Industrial Seeds, was boiled for 6 h, after which the titanium dioxide slurry was filtered and washed with deionized water to eliminate any soluble ions. The resulting white pulp was dried at 200°C for 48 h. Subsequently, it was ground and reslurried in deionized water to make up suspensions of various titanium dioxide concentrations (C = 40 g/L, 80 g/L, 120 g/L, and 240 g/L). Each suspension was stirred overnight to ensure homogeneity in particle-size distribution. We named this seed type Large Seeds top differentiate them from Industrial Seeds. The mean particle size of Large Seeds determined by laser diffraction (Coulter LS 230) was 1.36 μm. This particle size was maintained after inoculation into hot concentrated titanyl sulfate solution.

In each experimental run, the starting solution was heated to 100°C, after which seeds were inoculated. The precipitation run time was considered to be initiated once the last drop of seeds was added. The temperature was then raised at a rate of 1°C per minute to 110°C. All experiments were carried out at 110°C with stirrer speed maintained at 200 rpm.

A small sample (1–3 mL) was extracted at specific times, and quenched with 10% sulphuric acid (diluted from 98% Sulphuric Acid GPR, Merck) in an ice bath, for the determination of percentage recovery of titanium dioxide. These samples were centrifuged, after which the supernatant was carefully removed by pipette and the residue washed with the quenching medium. In carrying out this separation and washing routine a number of times, Fe^{2+} and other soluble impurities were eliminated from the wet anatase particles. Finally, the sample was oven dried and subsequently heated to 900°C before weighing. At 650°C, the sulphate ions attached on the surface of anatase particles were removed through the liberation of highly acidic sulphur trioxide fumes. This method enables us to accurately measure the total amount of anatase formed at a specific time of the precipitation run.

Samples, extracted using the procedure just given, were analyzed to determine the sizes of particles on the three relevant length scales; namely aggregates (1–2 μm), comprising agglomerates (60–100 nm), which are in turn made up of crystals (5–10 nm). The methods used to achieve this are now described.

PSDs of aggregates (particle of approximately 1–2 μm diameter) were obtained using an Elzone 280 PC with a 48 μm orifice tube. The Elzone 280 PC uses the principle of electrical zone sensing to count particles, and measures their size in terms of diameter of an equivalent volume sphere. Electrical-zone sensing directly counts numbers of particles: PSDs for the aggregates are therefore reported weighted by number and the mean size of aggregates is given as the number weighted mean diameter ($L_{1.0}$). Samples were taken from the stirred tank and subjected to the quenching procedures described earlier. Dilution of the sample in 40 g/L salt solution is required prior to particle-size analysis.

Aggregates were deaggregated into their composite agglomerates (agglomerates are approximately 60–100 nm in diameter), by treatment of anatase particles in 0.5 M barium chloride, according to the procedure described by Sathyamoorthy et al. (2001a). The mean size and PSD of primary agglomerates was then determined using a Coulter LS 230 machine working on the principle of laser diffraction, and measuring diameter of an equivalent volume sphere. Laser diffraction measures particle volume distribution: PSDs for the agglomerates are therefore reported as diameter distribution weighted by volume and the mean size of agglomerates is given as the volume-weighted mean diameter ($L_{4.3}$).

Dried samples were taken for powder diffraction studies (PXRD) to determine anatase crystal size. PXRD was carried out with a Philips (XRG 3100)/Stoe Powder Diffraction

Machine. The X-ray source was nickel-filtered copper $K\alpha$ radiation ($\lambda = 0.15418$ nm). The goniometer was operated under step scan mode in increments of 0.02° 2θ, and at a scanning speed of 0.01° 2θ per second. Diffraction peaks for titanium dioxide were identified with reference to JCPDS Powder Diffraction Files (1969). Crystal size was determined using Scherrer's formula (Hammond, 1997), shown in Eq. 4

$$\beta = \frac{K_S \lambda}{l \cos \theta}. \tag{4}$$

According to this formula, the line broadening or angular width at half maximum, β, is inversely proportional to the crystal size, l. The crystal size calculated in this way is a mean chord length in a direction normal to the crystal plane from which the diffraction line originates. In order to obtain a characteristic mean particle diameter from this, the shape correction factor, K_S, is introduced; for spherical particles this factor is about 0.9. Since we have no way of knowing the shape of the crystals present in our particles, we have taken this shape correction factor to be unity. Calculations were carried out on anatase peaks located at 2θ of 25.4°. The observed line broadening was corrected for "instrumental" factors by measuring the line broadening of large anatase crystals ($l = 265$ nm, Aldrich Chem. Co., 99.9% purity), and applying a simple subtraction to obtain the corrected line broadening ($\beta = \beta_{\text{observed}} - \beta_{\text{instrument}}$ (Hammond, 1997).

Quenched samples used for PSD measurements were filtered onto a 13-mm Whatman Cylopore membrane filter with 0.2-micron pore size. The membrane filters were air dried and adhered to aluminum mounting stubs with double-sided tape. These were gold coated in vacuum. A Joel JSM-820 scanning electron microscope (SEM) was used to observe changes in particle size and population.

Constant pressure filtration tests were carried out in a vertical acrylic pipe, 125 mm high and 75 mm ID. A Whatman 42 filter paper was held at the lower end of the pipe via a stainless-steel endcap. Compressed air entered the top of the pipe through a stainless-steel upper endcap. Anatase particles from a precipitation run were centrifuged and washed with a consistent amount of water (3 L). The anatase particles were then reslurried to appropriate concentrations for filtration tests. The pH value of the anatase slurry was measured using a Beckman 40 pH meter with a combination pH electrode. The pH of all anatase slurry used in the filtration experiments was between 1.0 and 1.2. As pH changes, the modulus of the zeta potential (which directly affects the particle–solution interaction) also changes. Since the objective in this work was to quantify the differences in filtration efficiency influenced by particle size alone, it was important that pH values did not differ significantly.

Filtration was carried out at 50–200 kPa for a range of slurry concentrations. A plot of cumulative volume of filtration vs. time was obtained using a stopwatch and measuring cylinder. Equations 2 and 3 were used to calculate a value of cake permeability for each sample analyzed. Filter-cake porosity and solidosity were determined by estimating the void fraction, from measurement of the water content of the cake; this method assumes the filter cake to be fully saturated, an assumption that is expected to be reasonable for cakes made up of particles as small as the ones in our samples. We first weighed the wet filter cake, and repeated the measurement after it has been dried at 105°C. Density of the fluid was taken as 1 $g \cdot cm^{-3}$, and density of the anatase particles as 4 $g \cdot cm^{-3}$ (Othmer, 1983).

Results

New seeding procedure

Influence of Large Seeds on precipitation. In the first set of experiments we varied the Large Seeds concentration. Inoculation of 59 mL of 40 g/L titanium dioxide corresponds to seeding of 1.8 wt. %. The use of 1.8 wt. % seeding is frequently encountered in industrial-scale processes.

The rate of precipitation is reported as percentage recovery of titanium dioxide (anatase) in Figure 1. Increasing the Large Seed concentration had little effect on the kinetics of the precipitation process: yields after 360 min were all between 33 and 39%. Recovery of titanium dioxide after 24 h for the 40-g/L seeding case was 87.3%. Comparison is made with a precipitation run where no seeds of any kind were inoculated. In this case, observable precipitation of anatase did not begin until the 90th minute; yield after 360 min was about 30%. Comparison with a precipitation run inoculated with 54 mL (1.8 wt. %) of Industrial Seeds confirms that the role of Large Seeds in promoting rapid precipitation of titanium dioxide was not significant.

The effectiveness of Industrial Seeds over Large Seeds in promoting the precipitation process and achieving high yield is probably due to two factors. The surface area in contact with titanyl sulfate solution is certainly one very important reason. The nature of the surface chemistry of seed particles

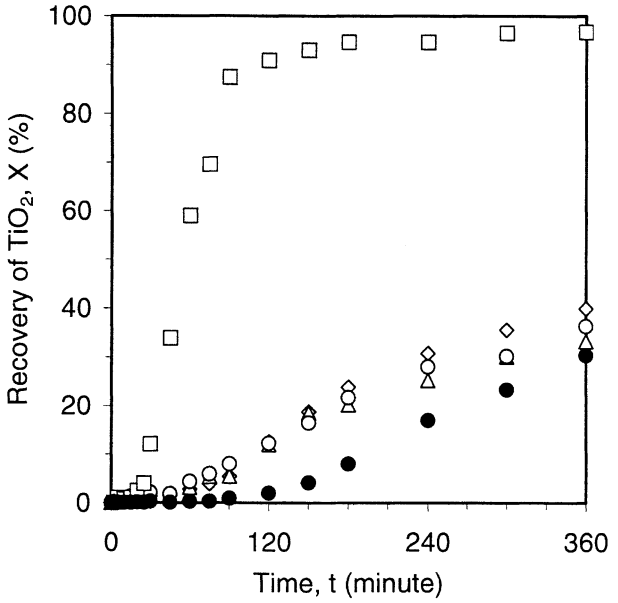

Figure 1. Recovery plots showing the influence of seeds on the kinetics of precipitation.

□: 54-mL Industrial Seeds 43.6 g/L (1.8% wt seeding basis); ◇: 59-mL Large Seeds 40 g/L (1.8% wt seeding basis); △: 59-mL Large Seeds 80 g/L; ○: 59-mL Large Seeds 120 g/L; ● nonseeded run.

is probably also a crucial factor, since all crystallization processes actually initiate in the gel form. Large Seeds have been dried at a temperature below that necessary for the liberation of sulfuric acid from the surface. The presence of this impurity might prevent the preferential formation of new nuclei on the surface of the seeds. Calcining the seeds at very high temperature causes phase transformation, from anatase to rutile. Therefore, we did not attempt to examine the use of calcined particles as seeding material.

Figure 2 illustrates the evolution of PSDs (measured using an Elzone 280 PC) with time, for runs inoculated with (a) 40 g/L (1.8 wt. %) (b) 80 g/L (3.6 wt. %) and (c) 120 g/L (5.4 wt. %) of Large Seeds with a constant inoculation volume of 59 mL. Consider first the case of the run inoculated with 40 g/L of Large Seeds (Figure 2a): the initial PSD of the seeds was clearly observable from the start. At the 120th minute, a bimodal distribution was recorded. A large number of particles smaller than the Large Seeds inoculated at the start of the experiment were present in the solution. It is likely that these smaller particles were formed directly from the solution, through the combined effects of homogeneous and secondary nucleation. The distribution of Large Seed particles

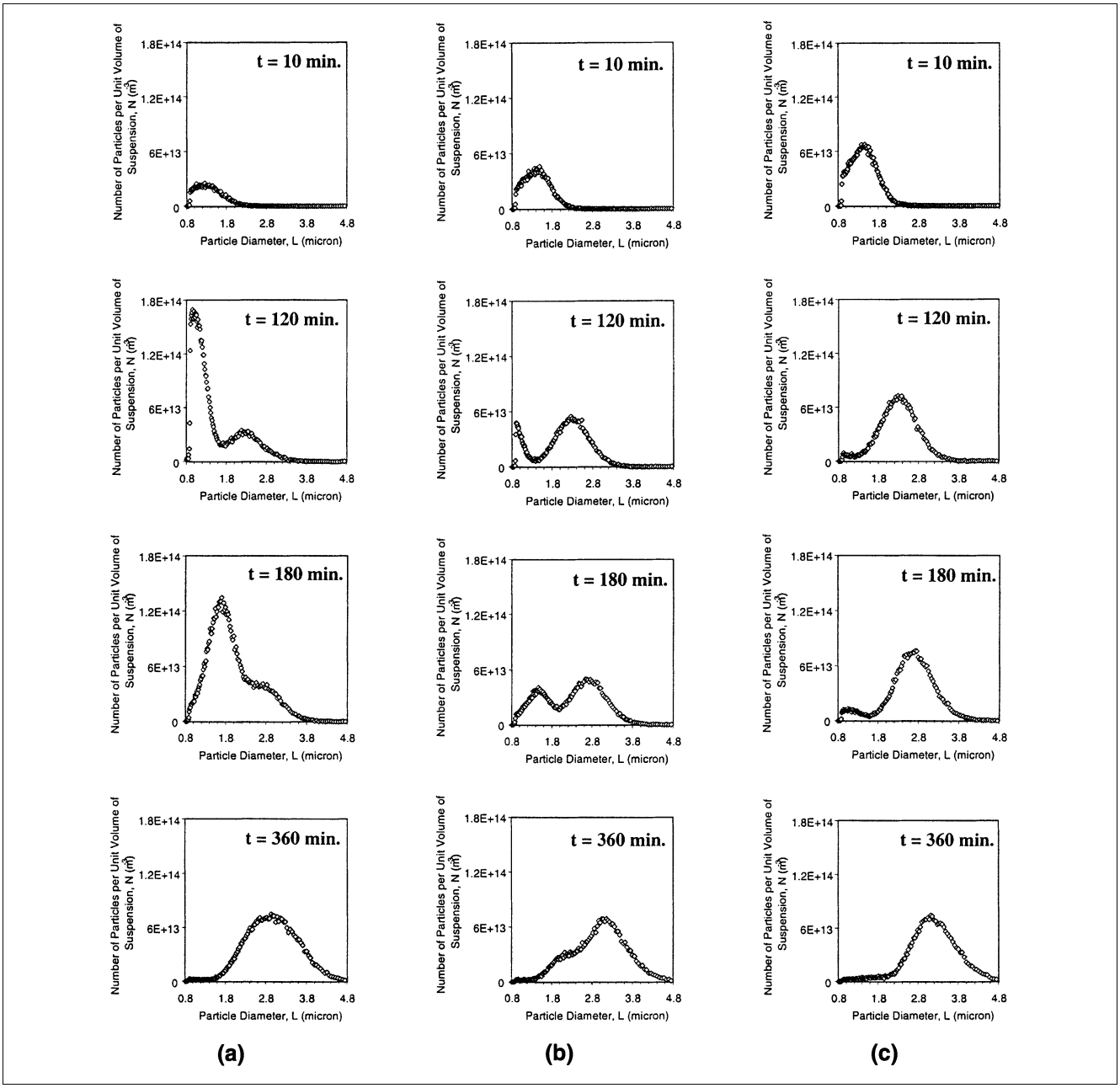

Figure 2. Evolution of aggregate size distribution (on a number-weighted basis) measured using an Elzone 280 PC with 19-μm orifice.

(a) Precipitation run inoculated with 59-mL Large Seeds (C = 40 g/L); (b) precipitation run inoculated with 59-mL Large Seeds (C = 80 g/L); (c) precipitation run inoculated with 59-mL Large Seeds (C = 120 g/L).

(the righthand lobe of the bimodal distribution), present from the start, remained visible but shifted to the right as the particles grew. By the 180th minute the PSD was less bimodal in appearance. The number of smaller particles that made up the lefthand side of the PSD has fallen. At the 360th minute, the PSD was no longer bimodal. A single population of large particles had evolved from the initially distinct Large Seed and smaller particle populations.

Similar observations were recorded for the case where 80-g/L Large Seeds were used (Figure 2b). However, the total number of particles that made up the smaller population of particles in the bimodal distribution at the 120th minute was much smaller.

In the case where the concentration of Large Seeds inoculated was 120 g/L (Figure 2c), the number of smaller particles making up the lefthand side of the PSDs at the 120th and 180th minute were reduced very significantly. As a consequence, these PSDs appeared almost unimodal. By the 360th minute, a unimodal PSD was observed with a slightly larger mean size than for the 40-g/L seeding case.

Data from the PSDs in Figure 2 are reported in terms of the total number of particles and mean particle sizes in Figures 3 and 4. Between the 120th and 240th minute, the population of larger aggregates (formed from the population of Large Seeds initially inoculated) in the bimodal distributions (see Figure 2) could be easily distinguished from the overall population. Therefore, we are able to report the total number and mean size of the larger aggregate population alone. In Figures 3 and 4 the fact that the total number of these larger aggregates remained constant throughout each precipitation run indicates that the larger aggregates were probably formed on Large Seed particles inoculated at the start. However, the size of these aggregates increased with time during precipitation.

Figure 3 also illustrates that when the concentration of Large Seeds inoculated is high (120 g/L), the total number of particles in solution remains almost constant throughout the precipitation process. This indicates that when a sufficient

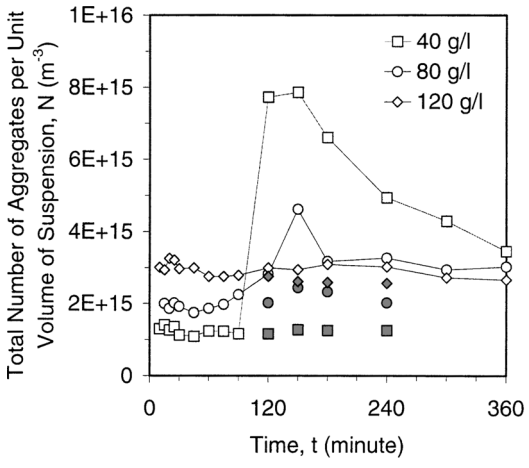

Figure 3. Change in the total number of aggregates in suspension with time for three different seed loadings of Large Seeds.

Shaded bullets represent values for the population of large aggregates only in the bimodal distribution (see Figure 2).

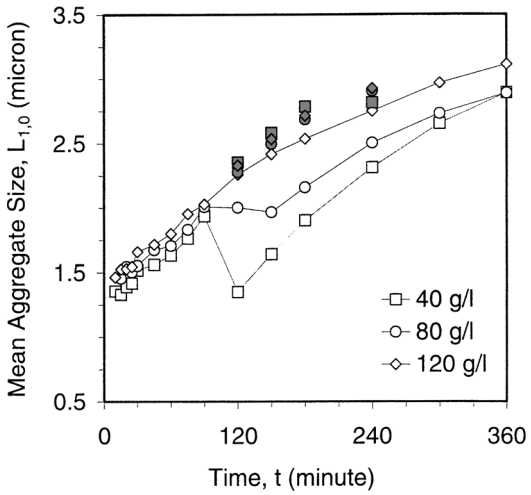

Figure 4. Diagram showing the change in mean aggregate size (on a number-weighted basis) with time for three different seed loadings of Large Seeds.

Shaded bullets represent values for the population of large aggregates only in the bimodal distribution (see Figure 2).

number of large particles is present in solution, all new agglomerates formed (by homogeneous or secondary nucleation) rapidly collide with and attach to one of these particles. Thus the population of smaller particles, which is "visible" at lower Large Seed concentrations, is very small and transient; all the smaller particles formed are rapidly scavenged by the large particles. The number of particles present remains constant at the number of Large Seeds initially added, and these increase in size both due to growth and aggregation with smaller particles.

In Figure 4 we observe that with the highest seed concentration a continuous increase in mean particle size occurred. The bimodal nature of the PSDs for runs inoculated with seeds of concentration 40 and 80 g/L TiO_2 resulted in a sudden drop in the measured mean particle size as the smaller particle distribution becomes "visible," around the 120th minute. For these two runs, a surge in the number of smaller particles was observed between the 90th and 240th minute.

The final mean aggregate size achieved using Large Seeds was between 2.7 and 3.2 μm.

SEM images taken at different times during precipitation runs provided further evidence for the formulation of a bimodal aggregate distribution. Figure 5 shows SEM images for one such run. A smaller aggregate population was observed along with the Large Seed particles at the 90th minute of precipitation. The population of particles remained segregated into two different distributions until the 180th minute. It can be seen that the Large Seed particles grew throughout the precipitation. In Figure 6, higher magnification shows that the enlargement of the seed particles was the result of aggregation between smaller aggregates and the Large Seeds. There is evidence, from Figure 6, that the smaller particles, aggregated on the surface of seed particles, continued to grow in size during precipitation. From the SEM image of aggregates at the sixth hour, we estimated the mean size of primary agglomerates to be between 200 and 300 nm. Crystal

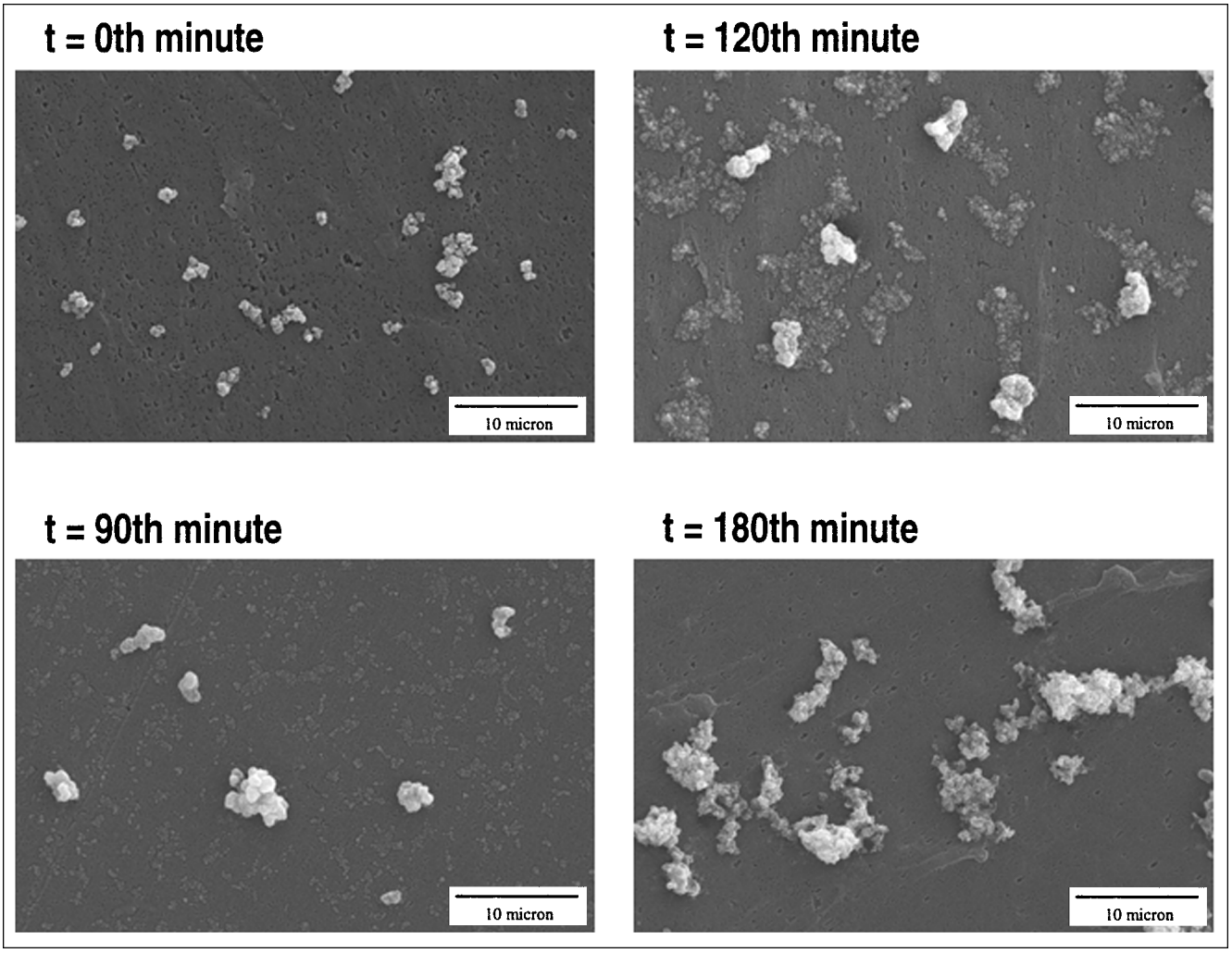

Figure 5. Scanning electron micrographs of aggregates in suspension for a precipitation run inoculated with 59 mL of Large Seeds ($C = 40$ g/L).

size for samples taken at the sixth hour was between 9 and 10 nm.

Although the effect on the overall kinetics of precipitation is insignificant, the addition of Large Seeds has a considerable influence on the population of particles in suspension. The Large Seed particles play the role of aggregation sites or "templates." The process of aggregation is aided by the presence of supersaturation. Supersaturation is required for growth and speeds the cementation of particles together. A higher concentration of particles in the solution also encourages aggregation by increasing the collision frequency. Therefore the number of smaller particles in the bimodal PSD for runs seeded with Large Seeds only was reduced significantly when a higher seeding concentration was used due to aggregation onto the Large Seeds. It might be possible to postulate the type of aggregation mechanism involved by solving population balance equations for the PSDs presented in this article.

Mixed Seeding. Experimental results in the previous section show that the presence of Large Seeds does not have a significant influence on the kinetics of precipitation. Industrial Seeds do increase the yield and rate of precipitation, but the mean aggregate size obtained using this seed type (Sathyamoorthy et al., 2001a) was only about 1 μm. Can the combined influence of both seed types be used to produce large aggregates and high yield? Two seeding procedures were investigated.

In the first seeding procedure, 59 mL of Large Seeds of concentration 240 g/L, and 20 mL of Industrial Seeds were added to the titanyl sulfate solution at the start of the experiment. We call this scheme the simultaneous seeding procedure (SSP). The second inoculation scheme is referred to as the controlled seeding procedure (CSP); 59 mL of Large Seeds of concentrations 240 g/L TiO_2 was added at the start of the experiment, together with 5 mL of Industrial Seeds. Subsequently, an additional 5 mL of Industrial Seeds was inoculated at each of the 30th, 120th, and 240th minutes of the experiment.

In both procedures we used Large Seeds at the concentration of 240 g/L TiO_2 because it was found that with lower Large Seed concentrations a bimodal aggregate-size distribution was observed during the entire precipitation process.

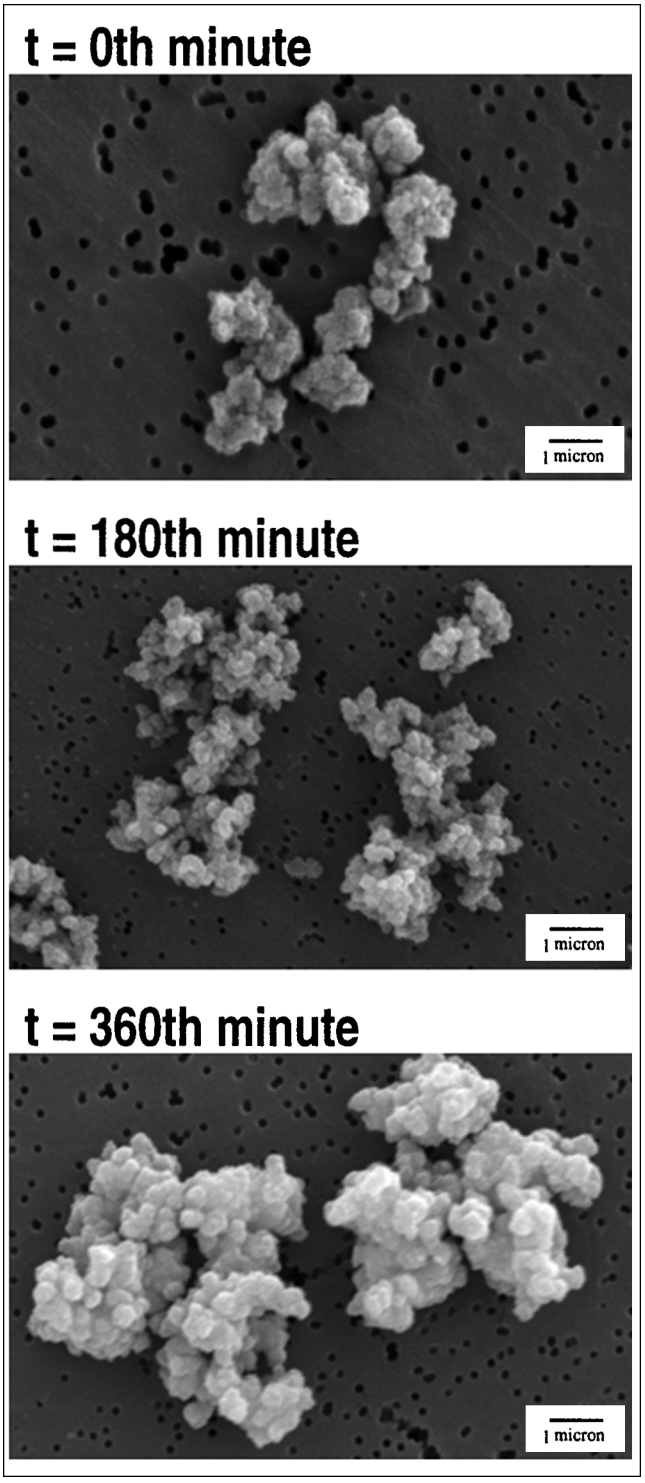

Figure 6. High magnification of aggregates showing the aggregation of smaller particles on the surface of Large Seeds.

Precipitation run inoculated with 59-mL Large Seeds; 40 g/L.

Note that this concentration of Large Seeds is twice that which was found adequate to give a unimodal distribution in the case where Large Seeds only were inoculated (see Figures 2–4). This is a result of the rapid secondary nucleation that is promoted by the presence of Industrial Seeds, causing fast production of smaller particles; a higher concentration of Large Seeds is required to provide sufficient aggregation opportunities to efficiently "mop up" these small particles.

For comparison purposes we carried out a precipitation run inoculated with only 20 mL of Industrial Seeds (ISO).

From the recovery plot in Figure 7, it can be seen that the addition of Industrial Seeds has a significant impact on the kinetics of precipitation. The maximum yield for all runs was almost identical, and closely resembled that achieved for ISO. For the SSP, there was initially a higher rate of precipitation because of the larger amount of seed present from the start. The initial rate of precipitation was slowest for the case of the CSP. This is not surprising since the amount of Industrial Seeds was increased gradually over a period of 4 h. However, final yield at the sixth hour was similar for all runs: between 90 and 95%.

In Figure 8, we present the evolution of PSDs with time for the two different novel seeding procedure and ISO. During the fifth minute, there were no obvious differences between the PSDs of the two different novel seeding procedures. In the case of ISO, no particles were observed at this time. At the 90th minute, we observed bimodal distributions for both novel seeding procedures, while a single population of particles was observed for ISO. The bimodal distributions were similar to those previously presented in Figure 2, but the total number of aggregates was about an order of magnitude greater. The presence of Industrial Seeds had significantly increased the rate of formation of new aggregates.

At the 360th minute, for the CSP, the shape of the bimodal distribution has changed, and has evolved into an almost unimodal distribution of particles, with large mean size. The

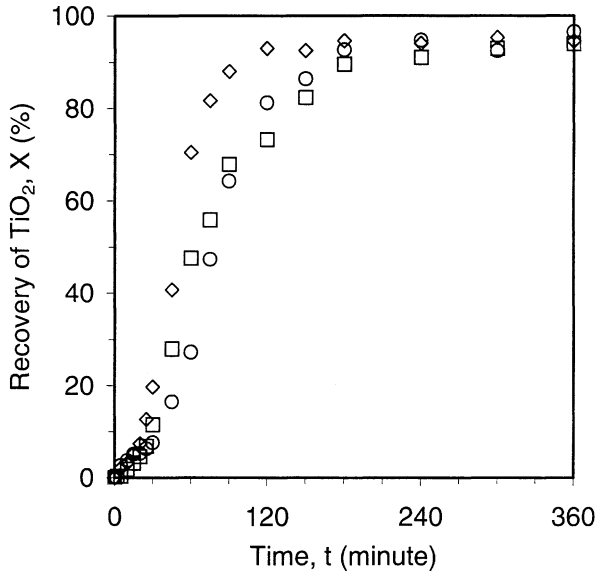

Figure 7. Recovery plots showing the influence of Industrial Seeds on the kinetics of precipitation for mixed seeding procedures.

Comparison is made with a typical industrial run (ISO) where only 20-mL Industrial Seeds (□) was used (◇: SSP; ○: CSP).

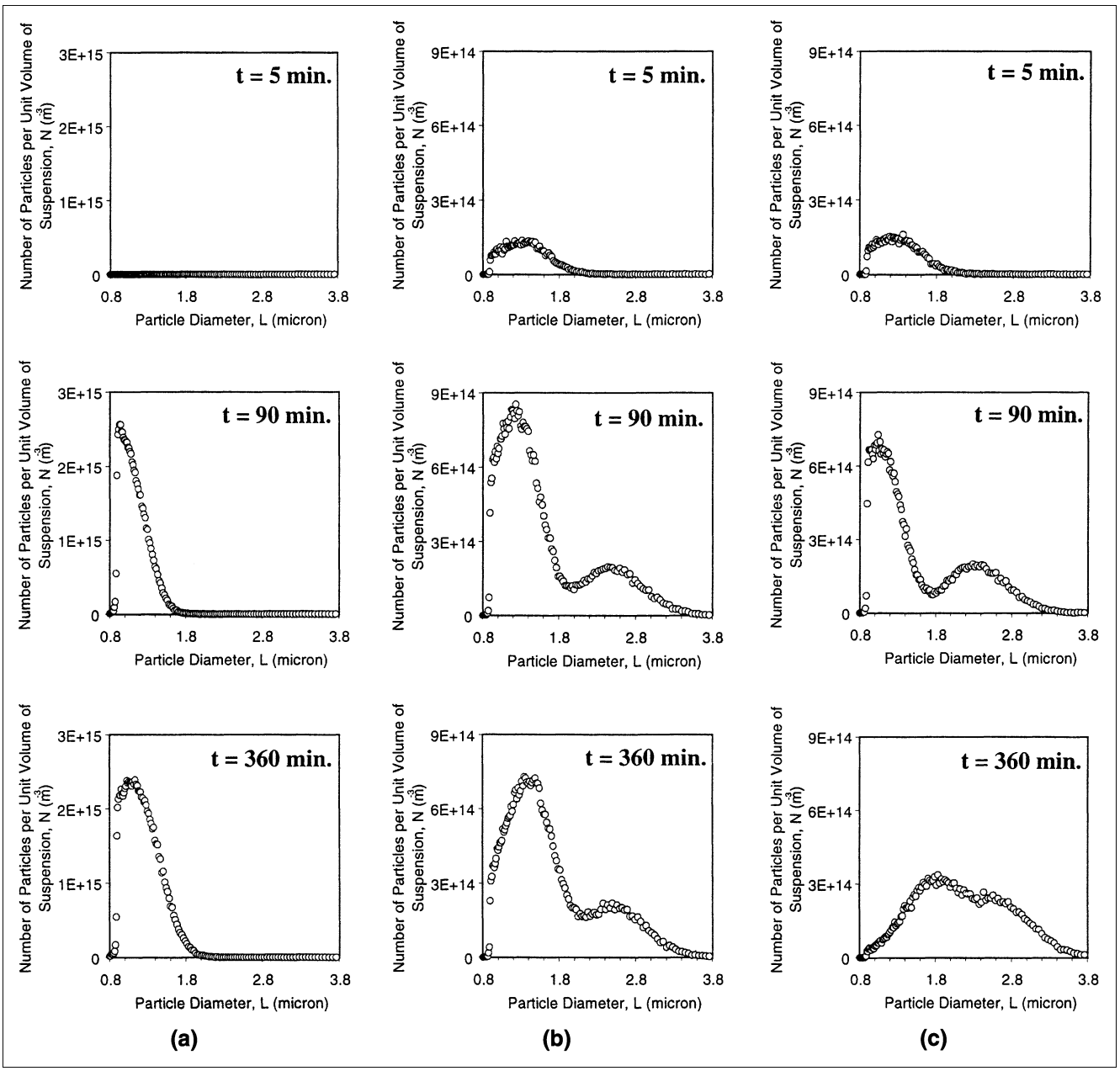

Figure 8. Evolution of aggregate size distribution (on a number-weighted basis) for (a) ISO; (b) SSP; (c) CSP.

shape of the bimodal distribution for the SSP remained almost unchanged at this time, indicating that the aggregates remained segregated into two populations. The smaller aggregates emerged from the solution due to the addition of Industrial Seeds, while the large aggregates were composed of particles formed on the Large Seeds. In the case of ISO, a single population of aggregates, with a much smaller mean size than that achieved using CSP, was recorded at the 360th minute.

The total number of aggregates and mean aggregate size were determined from the PSDs. The total number of aggregates in the large-sized aggregated distribution (the right-hand peak of the bimodal distributions), was always similar to the total number of Large Seed particles inoculated at the start. The role of Large Seeds is therefore to provide centers on which particles formed on Industrial Seeds can aggregate. There is little aggregation between particles growing on separate Large Seeds.

The total number of aggregates at the end of 6 h of precipitation was highest for ISO, followed by SSP and CSP, respectively. In terms of final mean aggregate size, the order is reversed, as is inevitable, since the total mass precipitated is constant. The mean aggregate size at the sixth hour for CSP was 2.13 μm, while for ISO the mean aggregate size was 1.15 μm. The mean aggregate size observed for the case of CSP was almost two times larger than that typically achieved in

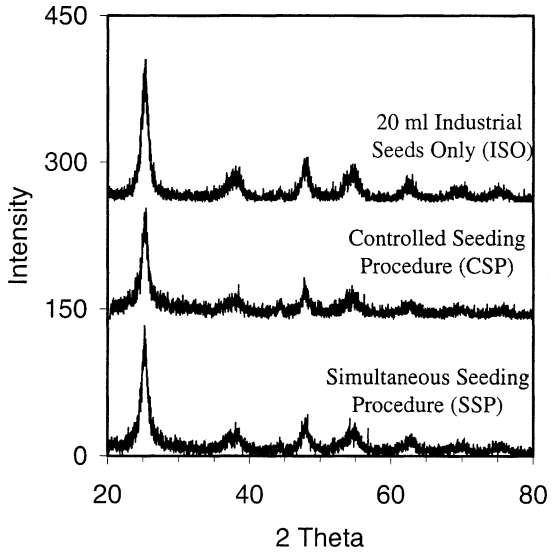

Figure 9. PXRD spectra for anatase samples taken at the sixth hour of precipitation.

All peaks shown in the diagram are anatase.

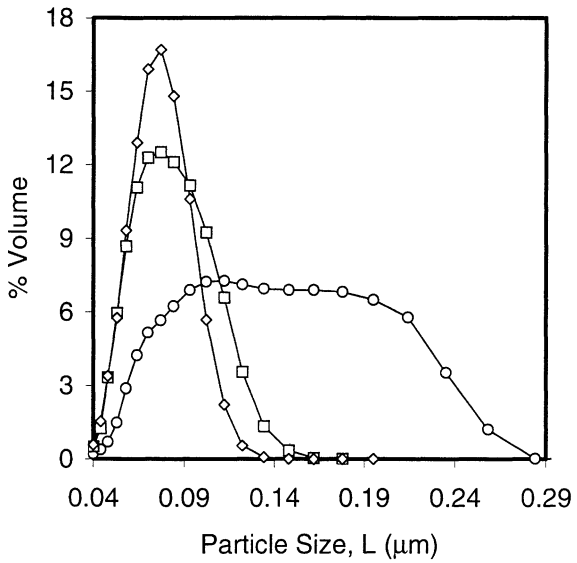

Figure 10. Size distribution (on a volume-weighted basis) of primary agglomerates at the sixth hour of precipitation measured after barium chloride treatment using a Coulter LS 230 (○: CSP; ◇: ISO; □: SSP).

the industry (Sathyamoorthy et al., 2001a). Mean aggregate size for SSP was 1.58 μm. However, the aggregate population in this case is bimodal with mode sizes of 1.45 and 2.50 μm for the segregated populations.

Figure 9 shows the PXRD patterns of samples from the three seeding procedures. It is noticeable how similar the three pattern are, indicating that the different seeding procedures have very little effect on the crystal size or morphology. Crystal size at the sixth hour for ISO was approximately 8.0 nm. In the cases of CSP and SSP, crystal size was about 8.5 and 8.6 nm, respectively. The error in these measurements is estimated to be around ± 1 nm, and so it can be concluded that the different seeding procedures have a negligible impact on the final crystal size.

The mean sizes of primary agglomerates were determined from the PSDs shown in Figure 10. Note that primary agglomerate size was measured using laser scattering, and is therefore reported on a volume-weighted basis (see Experimental section). The aggregate sizes reported in Figures 2–8 were measured using electrical zone sensing and are therefore on a number-weighted basis. Direct comparison therefore should not be made between either the PSDs or the mean particle sizes reported for aggregates and agglomerates. Volume weighting will always result in a higher figure for mean size than number weighting.

The mean primary agglomerate size for the case of ISO was 76.3 nm. In the cases of SSP and CSP, this value was 82.3 and 138.7 nm, respectively. The PSD for primary agglomerates in CSP was a broad distribution, compared to narrow distributions for SSP and ISO. It is believed that the particle size of anatase agglomerates is important in determining the final size of rutile particles after calcination, which gives the pigment its optical properties (Edwards, personal communication, 1999). Certainly the anatase agglomerates are in the correct size range to account for the final rutile particle size, which is a factor of 2–3 times larger. However, this is poorly understood and certainly no mechanism for such a link is well established. The extent to which the broader PSD of the primary agglomerates might affect the final pigments properties, via the rutile particle size, is unknown and beyond the scope of this study. It would be a fruitful area for future study.

When using mixed seeding procedures, the two seed types play different roles during precipitation. The Industrial Seeds are largely responsible for the enhanced precipitation of anatase, through the rapid formation of new particles. By contrast, the Large Seeds provide aggregation sizes. By controlling the inoculation of Industrial Seeds (CSP), the rapid depletion of supersaturation through the formation of new particles is suppressed. Supersaturation is constantly available for the formation of larger stable particles via aggregation. Consequently, a single distribution of larger particles can be obtained at the end of precipitation, produced by aggregation of the smaller particles onto Large Seed templates. The inoculation of a large quantity of Industrial Seeds at the start of the precipitation (SSP) results in a rapid loss of supersaturation, and inhibits the formation of stable aggregates when collisions occur. In both types of mixed-seeding procedures, the yield after 6 h is high, primarily because of the inoculated Industrial Seeds.

The mixed-seeding procedures maintain high yield and result in large aggregates (> 2 μm). Crystals are almost the same size after mixed-seeding precipitation as those obtained in industry (ISO). There are, however, marked differences in primary agglomerate size and population. In particular, mixed seeding allows a large increase in aggregate size to be achieved.

Filtration of anatase slurry

Filtrability. Cumulative filtrate volume was measured for anatase slurry from the different seeding procedures: CSP, SSP, and ISO. For each seeding procedure we carried out

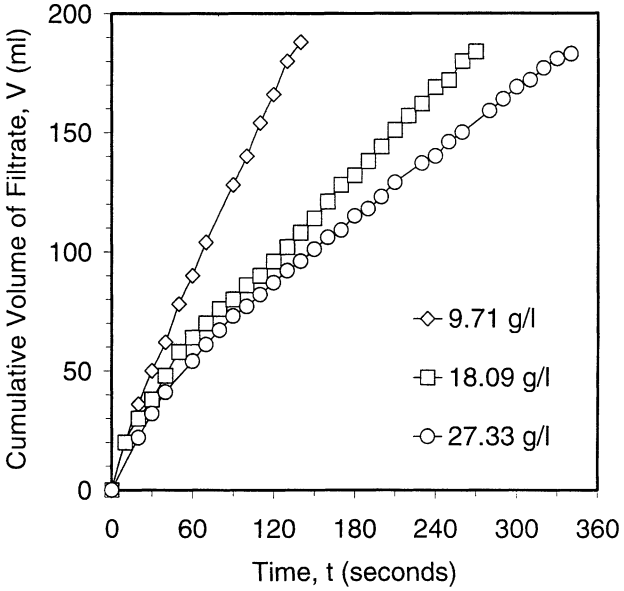

Figure 11. Volume of filtrate collected as a function of time for filtration of anatase slurry from the ISO method, carried out under constant pressure of 50 kPa.

Legend indicates anatase slurry concentrations.

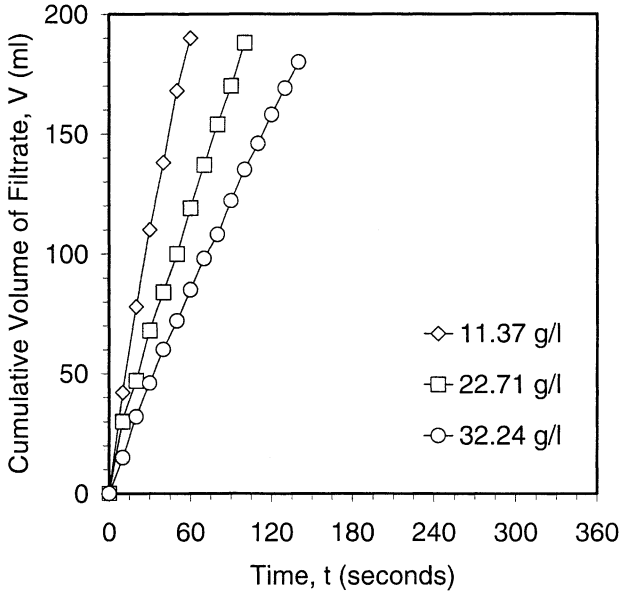

Figure 12. Volume of filtrate collected as a function of time for filtration of anatase slurry from the CSP method, carried out under constant pressure of 50 kPa.

Legend indicates anatase slurry concentrations.

filtration tests for three different concentrations of anatase slurry, in each case at filtration pressures between 50 and 200 kPa. Figure 11 shows the filtration test results for ISO. The rate of filtration starts to fall as the filter cake builds up.

With an increase in slurry concentration from 9.71 g/L to 27.33 g/L of anatase, there is a clear reduction in the filtration rate, due to the higher resistance from the thicker cake formed.

Figure 12 shows the same experiment, but for the case of anatase slurry from CSP. The most obvious difference between Figure 12 and Figure 11 is that the rate of filtration for the slurry from CSP was much faster compared to the slurry from ISO. This is believed to be due to the larger aggregate size in anatase from CSP. The difference between the filtration rate for ISO and CSP product was more pronounced when the slurry concentration was high.

Figure 13 shows the same filtration test results for anatase slurry obtained from SSP. Comparison between Figures 11, 12, and 13 shows that the filtrability of the slurry from SSP was intermediate between the other two slurries, as was its mean aggregate size.

As expected, an increase in filtrability of anatase slurry results from an increase in mean aggregate size in the slurry.

Cake Permeability. Whatman 42 filter paper used in our experiments has a mean pore size of about 2.5 μm. In the case of slurries from ISO and SSP, many of the anatase aggregates are less than 1.5 μm. During the early stages of filtration some of the solid particles can therefore pass through the filter paper. This stage occurs up to the point when about 50 mL of filtrate was accumulated. A steady state will only be reached once a consolidated cake has covered the filter medium. In light of this, we only analyzed data beyond 50 mL accumulated volume of filtrate. This stage was not observed for the slurry from CSP. It is likely that this was due to the larger mean aggregate diameter in this case.

Table 1 shows t_o, b, and c obtained from the Ruth relation for the highest slurry concentration tested for ISO (27.33 g/L), SSP (30.78 g/L), and CSP (32.24 g/L) at all pressures

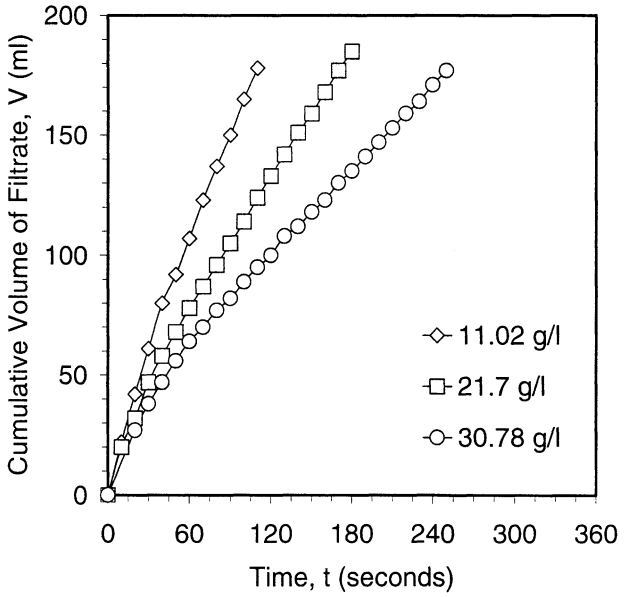

Figure 13. Volume of filtrate collected as a function of time for filtration of anatase slurry from the SSP method, carried out under constant pressure of 50 kPa.

Legend indicates anatase slurry concentrations.

Table 1. Data from Ruth's Equation and Analysis of Filtration Results Using Meeten's Method (2000) for Cake Permeability Values

Slurry/Pressure (kPa)	t_o (s)	b (smL^{-1})	c (smL^{-2})	Cake Solidosity, ϕ_{cake}	Mean Cake Solidosity, $\phi_{cake,mean}$	Solidosity of Slurry, ϕ	G	Permeab. y, $k \times 10^{-16}$ (m^2)
ISO (20-mL industrial seeds only) 20-mL industrial seeds $t = 0$ min								
Slurry concentration: 27.33 g/L								
50	−9.584	0.670	0.00633	0.1557				
100	−5.261	0.382	0.00398	0.1614	0.1624 ± 0.0050	0.00677	0.04351	6.800
150	−3.445	0.317	0.00288	0.1659				
200	−0.945	0.194	0.00214	0.1666				
SSP (simultaneous seeding procedure) 20-mL industrial seeds $t = 0$ min + 59 mL. Large seeds $t = 0$ min								
Slurry concentration: 30.78 g/L								
50	−7.767	0.612	0.00466	0.1824				
100	−1.458	0.418	0.00239	0.1857	0.1867 ± 0.0036	0.00762	0.04258	10.011
150	−0.756	0.255	0.00173	0.1877				
200	−0.662	0.134	0.00158	0.1910				
CSP (continuous seeding procedure) 5-mL industrial seeds $t = 0$, 30, 120, and 240 min. + 59 ML Large seeds $t = 0$ min								
Slurry concentration: 32.24 g/L								
50	−0.589	0.562	0.00159	0.2138				
100	−0.429	0.283	0.00087	0.2159	0.2168 ± 0.0040	0.00806	0.03859	25.366
150	−0.539	0.201	0.00069	0.2150				
200	−0.261	0.184	0.00052	0.2227				

tested. Figure 14 shows desorptivity, S, conforming to Eq. 2; the assumption of an incompressible cake appears to hold, that is, k is constant. Permeability, k, was calculated by assuming a constant value for cake solidosity, ϕ_{cake}, with varying pressure (see Table 1). Filtrate viscosity was taken as 0.001 Pa·s. Values shown in the last column of Table 1 indicate a permeability over three times higher for the filter cake formed by slurry from CSP than that formed by slurry from ISO.

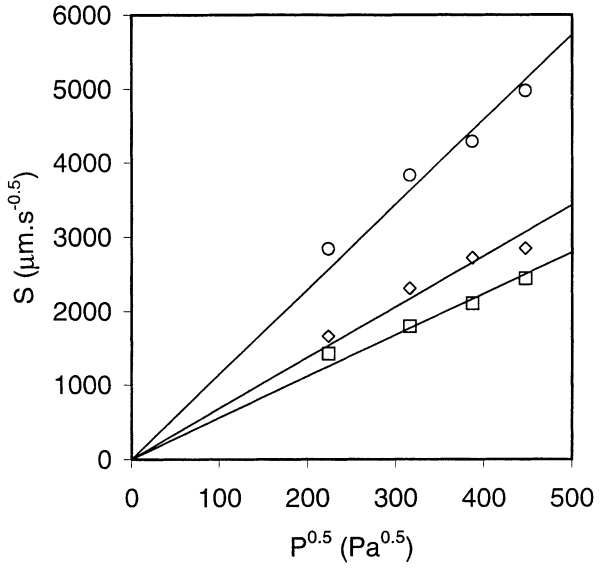

Figure 14. Plots showing relationship between desorptivity, *S*, and applied pressure, *P*, for anatase slurry from ISO, CSP, and SSP.

○: CSP slurry concentration of 32.24 g/L: ◇: SSP with slurry concentration of 30.78 g/L; □: ISO with slurry concentration of 27.33 g/L.

The difference in the mean aggregate size of the final product for ISO and CSP is approximately 1 μm. This difference has a tremendous effect on the filtration rate of the resulting anatase slurry. It is believed that smaller particles form a more compact cake, and this reduces dramatically the size of pores available for the flow of filtrate during filtration. Network formation in a filter cake could also determine its ultimate pore-size distribution, and this may not depend on size alone, but also on other physical and chemical properties of the solid particles. We have shown that slurry CSP has a marked advantage over a typical industrial case (ISO) in terms of filtration efficiency. In addition to the efficiency gain due to the improved cake permeability, it is likely that achieving larger aggregate sizes could reduce filtration costs in industry significantly by allowing the use of higher micron-rating filters than are currently used.

Conclusions

We have explored the possibility of using recycled titanium dioxide particles from previous precipitation runs as seeds in the recovery of titanium dioxide from fresh titanyl sulfate solution. It was found that such Large Seeds have an insignificant influence over the kinetics of the precipitation process. However, these seed particles serve as aggregation sites for smaller particles emerging from the solution. The resulting

particles were larger in size than those currently obtained in industry. In order to maintain a high yield of anatase, similar to that achieved industrially, the use of Industrial Seeds was necessary. Large Seeds were inoculated at that start of the experiment. By controlling the subsequent inoculation of Industrial Seeds over a period of time, it was possible to obtain final aggregates that were larger, but maintained the mean size of crystals and primary agglomerates close to the values obtained in industry.

This resulted in a faster filtration rate of the anatase slurry through the formation of a filter cake with higher permeability. The mixed seeding procedure proposed here may have the potential to enhance plant productivity through more efficient filtration of anatase slurry downstream of the precipitation process, while maintaining product quality and yield. The required process modification would be cheap and easy to implement.

Acknowledgment

The authors thank the Cambridge Commonwealth Trust and Hunstman Tioxide for financial assistance during the course of this research work. Advice on filtration by Gerry H. Meeten from Schlumberger Cambridge Research Ltd., and help from J. Edwards from Huntsman Tioxide on sulphate process technology is gratefully acknowledged.

Notation

A = area of filter medium, m^2
b = coefficient in Eq. 3, sm^{-3}
c = coefficient in Eq. 3, sm^{-6}
C = concentration of large seeds, gL^{-1}
G = (cake volume)/(filtrate volume) (see Eq. 2)
K = Kozeny coefficient
K_s = shape factor (see Eq. 4)
k = cake permeability, m^2
l = crystal dimension (see Eq. 4), nm
L = cake thickness, m
P = pressure, kPa
Q = cumulative filtrate volume per unit area of filter medium (see Eq. 1), m
R = filter medium hydraulic resistance (see Eq. 3), m^{-1}
S = desorptivity (see Eq. 2), $ms^{-1/2}$
t = time, s
t_o = time (see Eq. 3), s
V = cumulative filtrate volume, m^3

Greek letters

β = full width at half maximum of diffraction peak (see Eq. 4), rad
λ = X-ray wavelength, nm
η = filtrate viscosity, Pa·s
ϕ = solidosity
ϕ_{cake} = cake solidosity

Literature Cited

Akers, R. J., and A. S. Ward, "Liquid Filtration Theory and Filtration Pretreatment," *Filtration Principles and Practices*, Dekker, New York (1977).
Barksdale, J., *Titanium, Its Occurrence, Chemistry, and Technology*, Ronald Press, New York (1966).
Cain, C. W., "Putting the Principles to Work: Filter-Cake Filtration," *Chem. Eng.*, **97**(8), 72 (1990).
Chung, S. H., D. L. Ma, and R. D. Braatz, "Optimum Seeding in Batch Crystallisation," *Can. J. Chem. Eng.*, **77**, 590 (1999).
Duncan, J. F., and R. G. Richards, "Hydrolysis of Titanium(IV) Sulphate Solutions: 3. Properties of the Precipitated Solid," *N. Z. J. Sci.*, **19**, 185 (1976).
Hammond, C., *The Basics of Crystallography and Diffraction*, IUCr Texts on Crystallography, Vol. 3, Oxford Science Publications, Oxford, p. 146 (1997).
Koenders, M. A., and R. J. Wakeman, "The Initial Stages of Compact Formation from Suspensions by Filtration," *Chem. Eng. Sci.*, **51**, 3897 (1996).
Meeten, G. H., "A Dissection Method for Analysing Filter Cakes," *Chem. Eng. Sci.*, **48**, 2391 (1993).
Meeten, G. H., "Septum and Filtration Properties of Rigid and Deformable Particle Suspensions," *Chem. Eng. Sci.*, **55**, 1755 (2000).
Mydlarz, J., and A. G. Jones, "Continuous Crystallisation and Subsequent Solid-Liquid Separation of Potassium Sulphate Part II: Slurry Filtrability," *Chem. Eng. Res. Des.*, **67**, 294 (1989).
Othmer, K., *Encyclopedia of Chemical Technology*, Wiley, New York (1983).
Patton, T. C., *Pigment Handbook*, Wiley Interscience, New York (1973).
Ranjan, S., and R. Hogg, "The Role of Cake Structure in the Dewatering of Fine Coal by Filtration," *Coal Prep.*, **17**, 71 (1996).
Raskopf, G., and A. Gaunand, "Kinetics of Titanium Dioxide Precipitation from Titanyl Sulphate Solutions by Thermal Hydrolysis," *Proc. Eur. Cong. of Chem. Eng.*, Montpellier, France (1999).
Ruth, B. F., G. H. Montillion, and R. E. Montanna, "Studies in Filtration I. Critical Analysis of Filtration Theory," *Ind. Eng. Chem.*, **25**, 76 (1933).
Santacesaria, E., M. Tonello, G. Storti, R. C. Pace, and S. Carra, "Kinetics of Titanium Dioxide Precipitation by Thermal Hydrolysis," *J. Colloid Interface Sci.*, **111**, 44 (1986).
Sathyamoorthy, S., M. J. Hounslow, and G. D. Moggridge, "Particle Formation During Anatase Precipitation of Seeded Titanyl Sulphate Solution," *Cryst. Growth Des.*, **1**, 123 (2001a).
Sathyamoorthy, S., M. J. Hounslow, and G. D. Moggridge, "Influence of Stirrer Speed on the Precipitation of Anatase Particles from Titanyl Sulphate Solution," *J. Cryst. Growth*, **223**, 225 (2001b).
Svarosvky, L., *Solid-Liquid Separation*, Butterworths, London (1990).
Tioxide Group, *Manufacture and General Properties of Titanium Dioxide Pigments*, Tioxide Group Ltd., London (1992).

Manuscript received July 21, 2000, and revision received Apr. 2, 2001.